**International Conference on Space Optics—ICSO 2014**

La Caleta, Tenerife, Canary Islands

7–10 October 2014

*Edited by Zoran Sodnik, Bruno Cugny, and Nikos Karafolas*


# *Electro-optical characterization system develped for ATLIDCAS AIV: flat field and collimated beam injections*

*G. Ramos*

*H. Laguna*

*J. Torres*

*T. Belenguer*

esa icso proceedings cnes

International Conference on Space Optics — ICSO 2014, edited by Zoran Sodnik, Nikos Karafolas, Bruno Cugny, Proc. of SPIE Vol. 10563, 105635O · © 2014 ESA and CNES
CCC code: 0277-786X/17/$18 · doi: 10.1117/12.2304131

# ELECTRO-OPTICAL CHARACTERIZATION SYSTEM DEVELPED FOR ATLID-CAS AIV: FLAT FIELD AND COLLIMATED BEAM INJECTIONS.

G. Ramos[1,*], H. Laguna[1], J. J. Torres[2], and T. Belenguer[1].
[1] *INTA, Crtra. Ajalvir km 4, 28850 Torrejón de Ardoz, Madrid (SPAIN),* [2] *IberOptics, C/ Gamonal 16, Oficina 4 – 1, 28031 Madrid (Spain). Corresponding author: G. Ramos: ramoszg@inta.es.*

## I. INTRODUCTION

In the framework of the ESA EarthCare Mission [1], an atmospheric LIDAR (ATLID) was included as a payload [2]. CAS [3] is the co-alignment system of such a LIDAR instrument, the system responsible of guaranteeing the proper alignment of the projected laser beam and the reflected light collected. Within CAS, in which a consortium leaded by ASTRIUM France is working in, as well as CRISA (electronics) and LIDAX (mechanical engineering), INTA is in charge of the development of the instrumentation to be used on ground (on ground support equipments, OGSEs) needed for the proper electro-optical characterization.

The OGSEs are basically two: one for the flat filed injection (provided through an integrating sphere) and another one for the injection of a collimated beam (based on an off-axis parabolic mirror for its light injection path and a theodolite for its path used for the illumination direction determination), also with the capability of including a certain degree of divergence. Both are supplied by a UV (Ultra Violet) illumination system consisted on an UV LED (Light Emitting Diode) controlled through a LED driver also developed by INTA and compatible with the CAS instrument acquisition sequence.

Brief descriptions of these two OGSEs as well as a resume of its performances are reported on.

## II. OGSES DESCRIPTION

In the following lines, LED Driver Unit features and OGSE-1 and 2 descriptions are pretended to be provided.

### *A. LED driver*

The integrated circuit used for the peripherical driver developed for the high-current switching at very high speed required is the SN75451BP. In **Fig. 1** its schematic representation can be found, while in **Table 1** its switching characteristics are summarized.

Using the above described integrated circuit, the LED driver was configured as showed in **Fig. 2**.

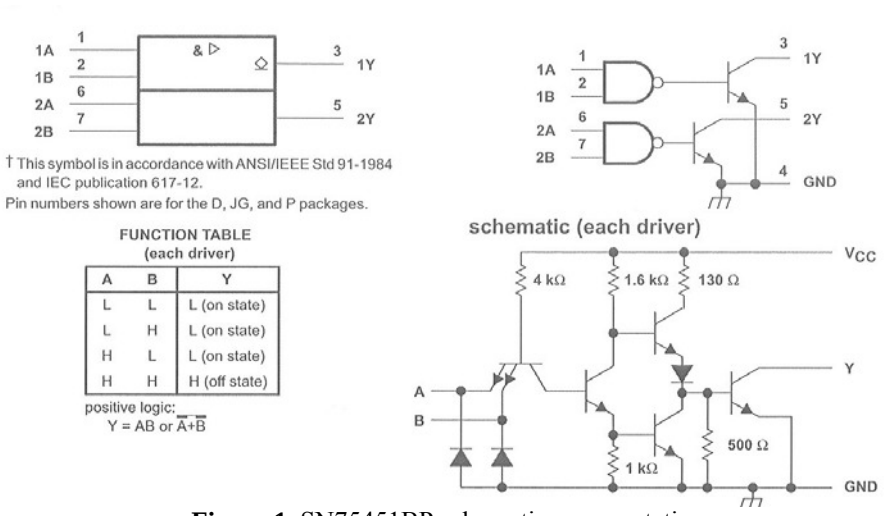


**Figure 1.** SN75451BP schematic representation.

**Table 1.** SN75451BP switching characteristics, $V_{CC}$ = 5V, $T_A$ = 25ºC.

| PARAMETER | | | TEST CONDITIONS | MIN | TYP | MAX | UNIT |
|---|---|---|---|---|---|---|---|
| $t_{PLH}$ | Propagation delay time, low-to-high-level output | | $I_O$ = 200 mA, $C_L$ = 15 pF, $R_L$ = 50 Ω, See Figure 1 | | 18 | 25 | ns |
| $t_{PHL}$ | Propagation delay time, high-to-low-level output | | | | 18 | 25 | |
| $t_{TLH}$ | Transition time, low-to-high-level output | | | | 5 | 8 | |
| $t_{THL}$ | Transition time, high-to-low-level output | | | | 7 | 12 | |
| $V_{OH}$ | High-level output voltage after switching | SN55451B | $V_S$ = 20 V, $I_O$ = 300 mA, See Figure 2 | $V_S$–6.5 | | | mV |
| | | SN75451B | | $V_S$–6.5 | | | |

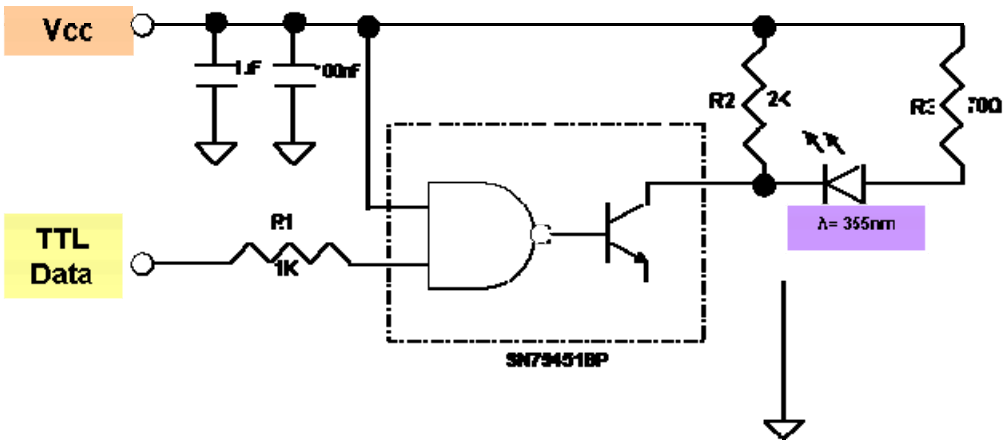


**Fig. 2.** LED driver: TTL shunt circuit based on an integrated circuit SN75451BP.

In the following lines, a brief description of its main characteristics can be found:

1. LED Driver switching characteristics ($V_{CC}$= 5 V, $T_A$= 25ºC):
   - Delay time, td: 22 ns
   - Storage time, ts: 64 ns
   - Rise time, ts: 20 ns
   - Fall time, tf: 4 ns
2. SNR (Signal to noise ratio):
   - SNR ≈ 160 (for 525nm LED)

*B. OGSE-1 (collimated beam)*

An ultraviolet LED (355 nm) will provide the proper wavelength light source. The LED light will be collected into the core (50µm) of an optical fibre (SMA/SMA connections). In order to optimize the coupling between the optical fibre and the LED a collimator constitutes of fused silica lenses in aluminium housing will be used.

The output of the optical fibre is located in the focal point of an off axis parabolic mirror which EFL (Effective Focal Length) is 134 mm (Edmund NT90-976, high performance off-axis parabolic mirror). The fibre output location will be adjusted by means of a positioning system (x-y-z adjustable). The positioning system has two functions: to locate the fibre output at the off axis parabolic mirror focal point in order to generate a collimated beam and to provide the translation movement that will allow modifying the divergence degree as required for the input beam at the CAS entrance pupil.

The VIS channel of the OGSE 1 consists of a theodolite. Such a channel is also directed to CAS through a beam splitter cube in order to measure the injection light direction with respect to a CAS proper optical reference surface (or whatever other optical reference required for injection direction determination).

The CAS entrance pupil (EP) will be defined by a mechanical stop manufactured in Delrin (Ø = 20.7mm). All the elements that constitute the OGSE 1 will be conveniently baffling in case to be necessary to avoid OGSE 1 stray light affects to CAS.

A director mirror will allow pointing both the collimated beams (the UV injected and the VIS corresponding to the theodolite) into CAS entrance.

The monitoring of the light signal will be made at CAS entrance by means of a Newport power meter model 918D-UV.

The main optical characteristics of the OGSE 1 elements are listed below:

- Off axis parabolic mirror EFL: 134 mm.
- Mirrors coating: Mg2Al
- Optical fibre NA: 0.22
- Optical fibre core diameter: 50 µm.
- Theodolite Leica T3000 (The OGSE 1 optical axis height is defined by the theodolite optical axis height that is 235 mm)

The schematic representation as well as a picture can be found in **Fig. 3**.

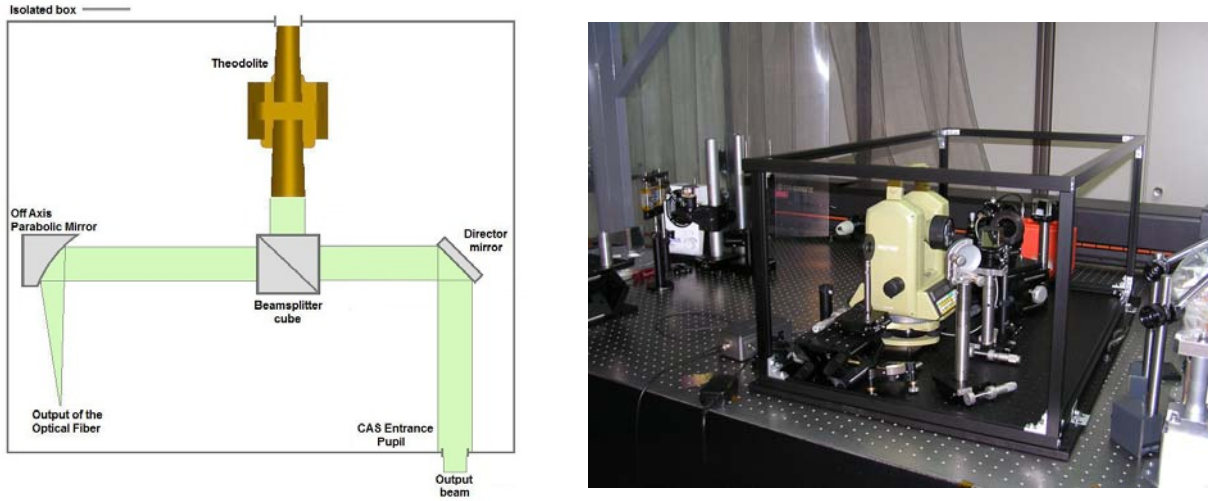


**Fig. 3.** OGSE-1 schematic representation (left) and real picture (right).

*C. OGSE-2 (flat field)*

This OGSE will basically consist on a 2" diameter integrating sphere with an aperture of 3.2 mm. The light source that feed the integrating sphere can be selected. A 355nm LED or a monochromator (only in the spectral response test) are available. The output of the integrating sphere is located at the off axis parabolic mirror focal point. The integrating sphere is mounted on a series of positioning subassemblies that allow its alignment with respect to the parabolic mirror (x,y,z adjustable).

In case to be required (i.e. if the LED power supply regulation is not enough) after the parabolic mirror, a filter wheel can be included in order to select the light levels available for the response linearity test. As in OGSE 1, a director mirror will allow pointing the beam in the OA (Optical Assembly, element at the entrance of the CAS instrument) entrance. The last element of the OGSE 2 is the CAS entrance pupil with a diameter of 20.7 mm.

The monitoring of the light signal will be made at CAS entrance by means of a Newport power meter model 918D-UV.

The schematic representation as well as a picture can be found in **Fig. 4**.

III. OGSE CHARACTERIZATION

*A. LED driver – UV (355nm) LED*

1. Power stability.

Different supplied powers were considered. The LED driver allows selecting the power at which the LED is supplied. In particular, there are two fixed modes, the low-power regime and the high-power regime, depending on the voltage that is applied to the LED. For both of them, then the voltage can be finely modified by a potentiometer. In this section, the emission stability results for two different applied voltages within the low-power regime are reported on.

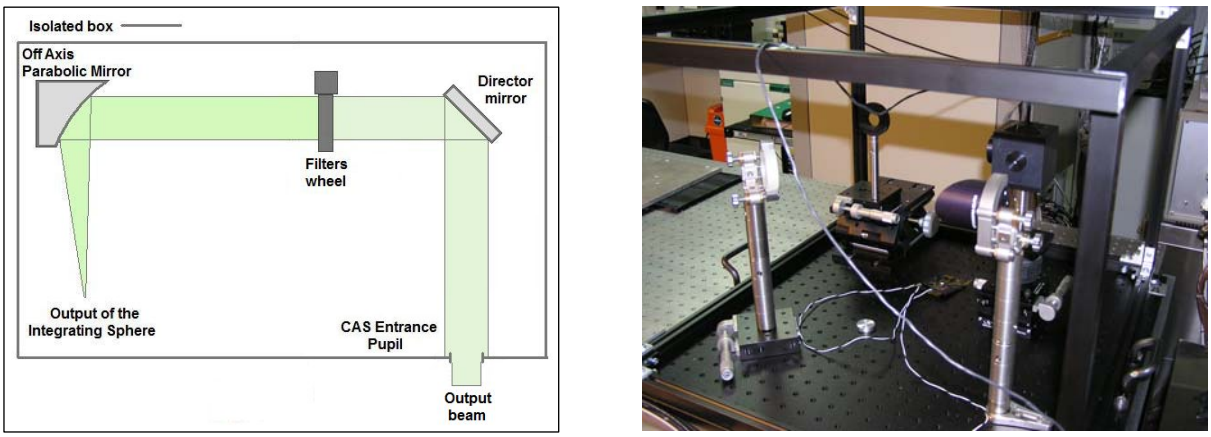


**Fig. 4.** OGSE-2 schematic representation (left) and real picture (right).

1.a) *LED driver at its maximum in 'low-power regime'.*

Once LED was properly located in front of the element used as collimator, and such element properly located with respect to the fibre collector, LED driver was switched on and measurements at the fibre output were started to be taken. **Fig. 5** shows the power evolution with time at the fibre output when the LED driver is commanded in 'low-power regime' at its maximum.

As can been observed, considering around the first hour of the LED function from the switching on, and taking into account the minimum and maximum power values, the difference was ≈1.4%/1hour.

After two hours from the LED switching on, power time evolution was measured again during one hour. Considering only the stability during one hour after these warming-up two hours (**Fig. 6**), both the averaged value as well as the standard deviation were computed, obtaining: $P = 6.917 \times 10\text{-}5 \pm 3 \times 10^{-8}$ W (≈ 0.04%).

In addition to the averaged value (and the associated standard deviation), and taking into account the lowest and highest values, the variation in such a worst case is around 0.3%/1 hour.

1.b) *LED driver at one intermediate applied voltage in 'low-power regime'.*

In order to check the light power regulation LED driver capability, one intermediate voltage was applied to the LED driver and after a warming up process, the power time evolution at the fibre output was measured. **Fig. 7** shows such evolution.

After around three hours from the LED switching on, but just exactly after the modification of the LED power supplied, the power time evolution was measured. Considering the lowest and highest values, the variation in such a worst case is around 1.1%/1 hour.

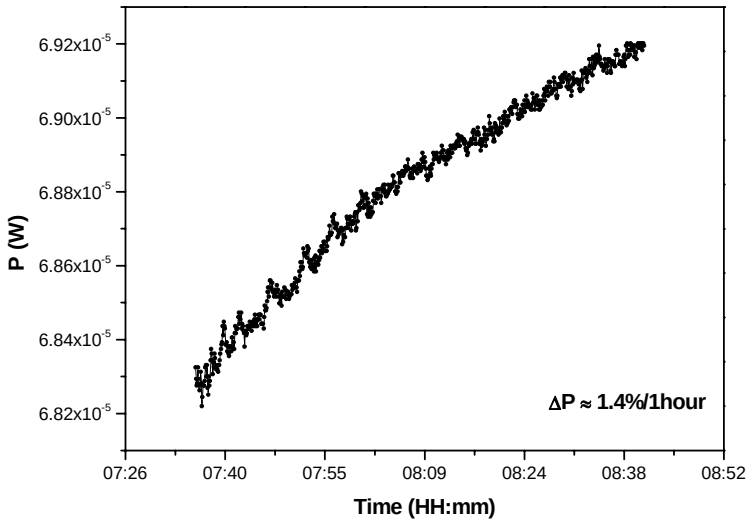


**Fig. 5.** UV LED power time evolution at fibre output (LED driver 'low-power regime' mode maximum).

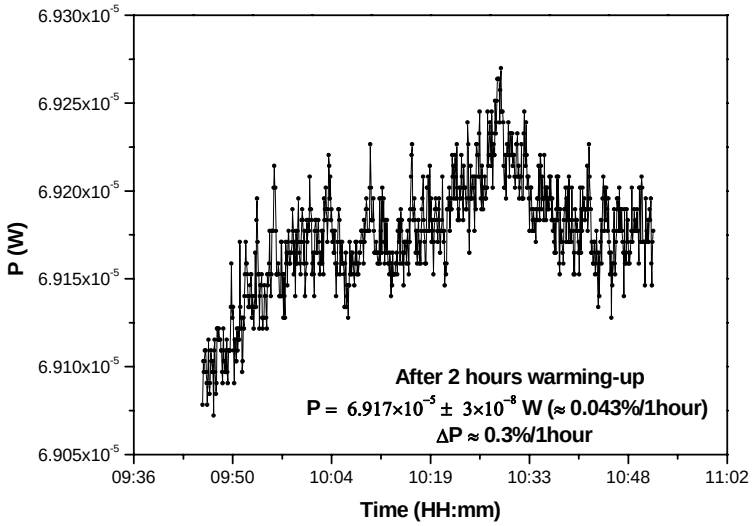


**Fig. 6.** UV LED power time evolution at fibre output after around 2 hours of warming up (LED driver 'low-power regime' mode maximum).

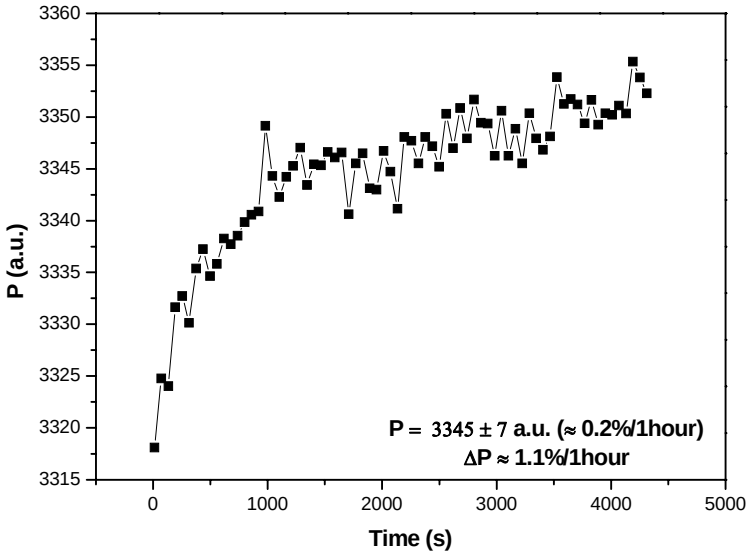


**Fig. 7.** UV LED power time evolution at fibre output after around 3 hours of warming up (intermediate value of the LED driver 'low-power regime' mode).

2. Wavelength stability.

Once the intermediate voltage mentioned in the previous section was applied to the LED driver, the LED emitted wavelength (λ) stability was investigated.

Attending to the fibre output measurement taken through a portable spectrometer (Ocean Optics HR2000CG-UV-NIR). As can be observed, the λ value for the LED peak emission is: $\lambda_{peak} = 353.1 \pm 0.5$ nm (0.14%), which is coherent with the LED specified value (353nm).

*B. OGSE-1 (collimated beam)*

1. Spot size.

In order to evaluate the expected spot size corresponding to the OGSE-1 injection, a proper set-up was prepared. It basically consists on the OGSE-1 but locating after the beam-splitter a high optical quality doublet of 250mm of focal length. The image will be then formed on a CCD (Imaging Source DMK 41BUC02). This camera was chosen due to its characteristics. The DMK 41BUC02 is a monochromatic camera (without bayer filter) with sensitivity enough in the UV range (particularity for 351nm) to obtain an image of the OGSE-1.

Considering the focal length ratio of the parabolic mirror and the doublet, M ≈ 1.85. The core diameter of the optical fibre is 50 μm, so the spot size should be about 93μm.

The beam was focused through the lens and directed to the CCD. The diameter of the spot is 19pixels. The CCD of this camera has a unit cell size of 4.65x4.65μm$^2$, then the spot size area is about 88.4μm. The theoretical value for 93μm would be 20pixels, which is close to the obtained value. The spot images obtained with different exposure times are shown in the **Fig. 8**.

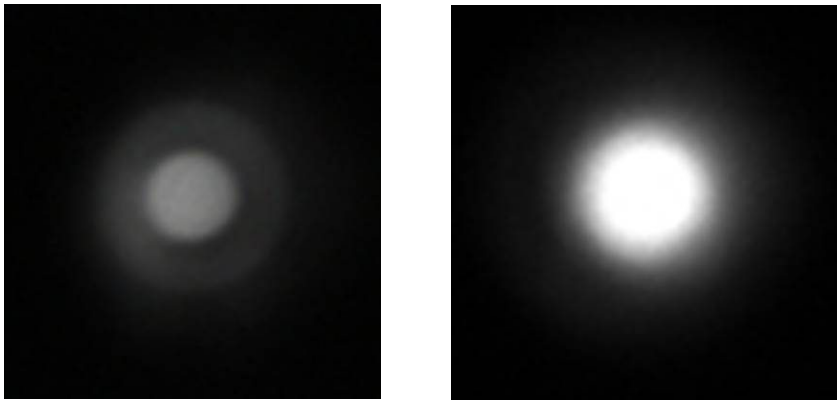

**Fig. 8.** The Spot of UV LED beam at the output of beam-splitter cube. The spot diameter is about 19 pixels (right size image corresponds to a higher exposition time acquisition than the left size one).

As CAS lens (EM and PFM) has a f ≈ 41.3mm therefore M ≈ 0.3. So when the beam pass through this lens, the expected diameter of the image formed on the MCCD would be about 15μm (for a perfect lens) regardless the lens aberration that will increase such a spot image diameter.

2. CAS EP radiometry (OGSE-1).

OGSE-1 injected irradiance at CAS Entrance (and at CAS Entrance Pupil, TBC) is pendant to be measured.

As will be demonstrated with the measurements corresponding to the OGSE-2 (next section), the OGSE output stability is basically dominated by the LED driver. So it can be concluded that it is always around 1%/hour

*C. OGSE-2 (flat field)*

1. Flat field homogeneity.

In order to evaluate the FFH (flat field homogeneity), several measurements of the power (and irradiance) are carried out in different sub-pupils of the entrance pupil. **Table 2** shows the measured values.

System characteristics:

- Sub-pupil size: 0.8350 $cm^2$ (circular)
- EP size: Ø = 20.7 mm
- A fine scanning of the EP is done as follow: Five areas moving the detector (sub-pupil) on X, and Y coordinate axis were analysed by doing three measurements in each area.

As a result, it can be concluded that the flat field (FF) and homogeneity (H) values are: FF = (5.71 ± 0.08) nW; H = 1.4%.

2. CAS EP radiometry (OGSE-2).

2.a) *White illumination*.

**Fig. 9** shows the time evolution of the power measured at CAS EP when the integrating sphere is supplied by a white lamp directly in front of its biggest port. Considering such a Fig., both the averaged value as well as the standard deviation were computed, obtaining: $P = 9.293\times10^{-7} \pm 7\times10^{-10}$ W (0.08%).

2.b) *UV (353 nm) LED illumination*.

**Fig. 10** shows the time evolution of the power measured at CAS EP when the integrating sphere is supplied by a UV led directly coupled to its biggest port. Again considering such a Fig., both the averaged value as well as the standard deviation were computed, obtaining: P = 175 ± 2 pW (1.14 %).

**Table 2.** Measurements of the power in different sub-pupils of the entrance pupil.

| Measure | Average (nW) | Standard Desv. (nW) |
|---|---|---|
| Centered | 5.71 | 0.04 |
| +ΔX | 5.69 | 0.09 |
| -ΔX | 5.58 | 0.06 |
| +ΔY | 5.80 | 0.10 |
| -ΔY | 5.77 | 0.03 |
| **Total** | **5.71** | **0.08** |

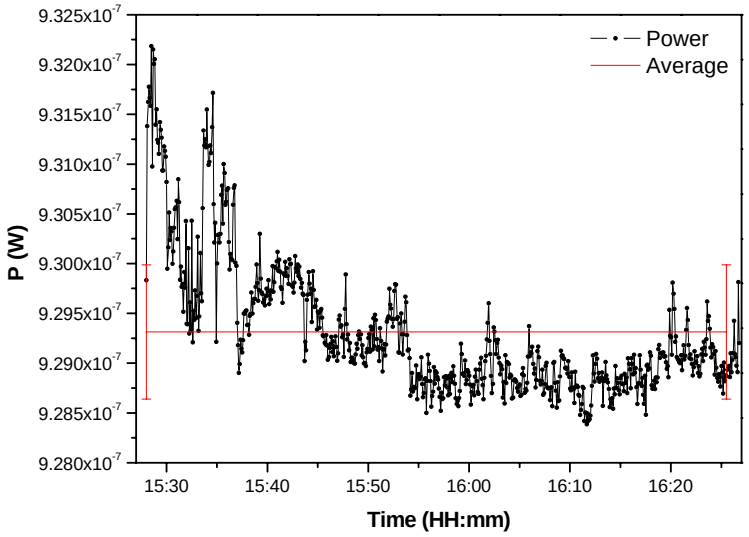


**Fig. 9.** CAS EP power time evolution measured when a white lamp is supplying the integrating sphere.

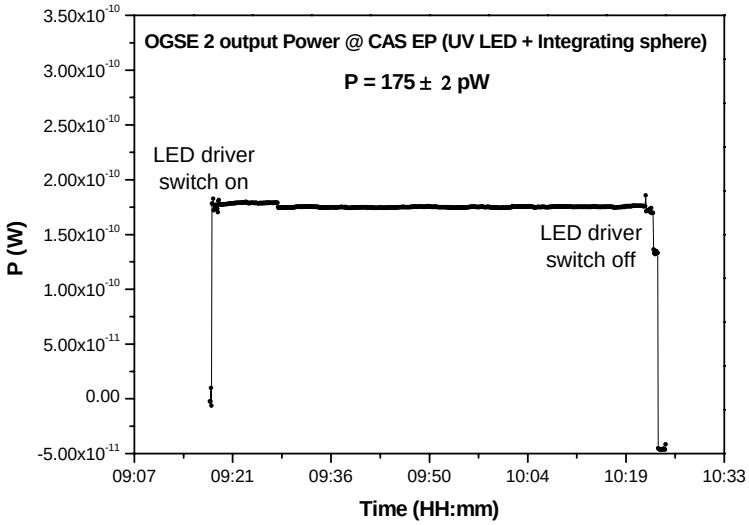


**Fig. 10.** CAS EP power time evolution measured when a white lamp is supplying the integrating sphere.

## IV. CONCLUSIONS

Two OGSEs have been developed for ATLID-CAS electro-optical characterization, including a LED driver allowing proper synchronization with the electrical signal coming from the acquisition sequence provided by CRISA at system level.

The performances found for the OGSEs in terms of synchronicity, amount of light and stability permit to assure that they are the proper ones for a further ATLID-CAS electro-optical characterization.

## V. ACKNOWLEGDMENTS

Authors thank to all the CAS consortium members (from ASTRIUM France, CRISA Spain, and LIDAX Spain) for his help and valuable opinions. Authors also thank to Instituto Nacional de Técnica Aeroespacial (INTA) for its support.

## VI. REFERENCEES

[1] P. Ingmann, “Reports for Mission selection. The six candidate earth explorer Missions”, ESA SP-1279 (1), April 2004, ISBN 92-9092-962-6.

[2] A. Hélière, R. Gelsthorpe, L. Le Hors, Y. Toulemont, "ATLID, the Atmospheric Lidar on board the EarthCARE Satellite", Proceedings of the ICSO (International Conference on Space Optics), Ajaccio, Corse, France, Oct. 9-12, 2012, paper: ICSO-065.
[3] D. Morancais, R. Sesselmann, G. Benedetti-Michelangeli, M. Hueber, "The atmospheric Lidar instrument (ATLID)", Acta Astronautica, Elsevier, Volume 34, Pages 63–67, October 1994.